

Bimolecular recombination losses in polythiophene: Fullerene solar cellsC. G. Shuttle,¹ B. O'Regan,¹ A. M. Ballantyne,² J. Nelson,² D. D. C. Bradley,² and J. R. Durrant^{1,*}¹*Department of Chemistry, Imperial College London, South Kensington SW7 2AZ, United Kingdom*²*Department of Physics, Imperial College London, South Kensington SW7 2AZ, United Kingdom*

(Received 4 April 2008; revised manuscript received 19 June 2008; published 9 September 2008)

Transient absorption spectroscopy is employed to monitor charge carrier decay dynamics in an annealed poly(3-hexylthiophene): methanofullerene solar cell. Comparisons of device and film data and data under applied bias demonstrate that these dynamics are dominated by bimolecular recombination. These data allow us to quantify the rate constant for bimolecular recombination, found to be strongly carrier density dependent, and thus determine the bimolecular recombination flux. By comparison with the device short-circuit photocurrent we conclude that the open-circuit voltage is primarily limited by bimolecular recombination.

DOI: 10.1103/PhysRevB.78.113201

PACS number(s): 73.50.Gr, 73.50.Pz, 73.61.Ph, 73.61.Wp

Organic solar cells based on polymer:fullerene blend films are attracting extensive interest for potential low cost solar energy conversion, with power conversion efficiencies (PCEs) now exceeding 5%.^{1,2} A key advance in the development of organic solar cells was the introduction of donor:acceptor blend films, or “bulk heterojunctions,” which enable efficient exciton diffusion to the charge separation interface. However, a drawback of such intimate mixing of donor and acceptor material is that photogenerated charge carriers may be lost via interfacial bimolecular recombination:

$$\frac{dn}{dt} = -knp, \quad (1)$$

where n and p are electron and hole carrier concentrations, respectively, t is time, and k is the bimolecular recombination coefficient (or “rate constant”).

There have been extensive studies of the importance of bimolecular recombination in limiting the performance of organic bulk heterojunction solar cells, focusing in particular on devices based on poly(3-hexylthiophene) (P3HT): 1-(3-methoxycarbonyl) propyl-1-phenyl-[6,6]-methanofullerene (PCBM) blend films. However, quantification of magnitude of bimolecular recombination losses in such devices remains controversial. It has, for example, been reported that the bimolecular recombination coefficient for P3HT:PCBM devices is several orders of magnitude smaller than predicted using a Langevin description, suggesting that bimolecular recombination may be unimportant in such devices.^{3–5} This contrasts with analyses of device current voltage data which have typically been indicative of significant bimolecular recombination losses.^{6,7} One complication with experimental studies to date is that they have all been based on optoelectronic studies of complete devices, where interpretation of the data is complicated by the range of other processes which may contribute to charge carrier losses in addition to bimolecular recombination (e.g., short circuits and device shunts, recombination at device electrodes, electric field dependent geminate recombination, etc.) or under conditions which are difficult to relate directly to device photovoltaic performance under solar irradiation.^{8–10} Herein we employ an all optical technique, transient absorption spectroscopy (TAS), to monitor charge carrier decay dynamics both in thin P3HT:PCBM

blend films and complete P3HT:PCBM devices. We have previously used this technique to monitor polaron decay dynamics in a range of polymer:PCBM thin films.^{2,11,12} By comparison of film and device data, and by consideration of data collected under applied bias, we conclude that the charge carrier decay dynamics at an open circuit in the P3HT:PCBM devices studied herein are indeed dominated by bimolecular recombination. These decay dynamics are shown to exhibit an approximately third-order dependence upon charge density found ($dn/dt \propto n^3$), in agreement with our previous transient optoelectronic analyses.^{13,14} Analysis of these dynamics in terms of bimolecular recombination allows us to quantify a carrier dependent bimolecular rate coefficient $k(n)$. We thus obtain an estimate for the overall bimolecular recombination flux under device operation, and by comparison with the device photocurrent, conclude that the device open-circuit voltage (V_{oc}) is primarily limited by this bimolecular recombination process.

Transient absorption spectroscopy is an all optical technique which monitors the change in optical density (ΔOD) of a sample upon pulsed photoexcitation due to the generation of transient species. As such it is a “contactless” technique and can therefore be employed both on complete devices and on the photoactive layer in the absence of electrodes. Due to the opacity of the metal contact, device data must be collected in reflection mode. A 100 mW, 980 nm laser diode probe was used to monitor absorption of the P3HT⁺ (Ref. 15) polarons generated using a nitrogen laser pumped-dye laser as an excitation source (λ_{exc} 520 nm, freq. 4 Hz, pulse duration <1 ns, intensity 4–60 μJcm^{-2}). Studies were performed on devices fabricated as detailed previously,² consisting of a 170 nm thick 1:1 blend film of regioregular P3HT and PCBM, spin-coated on top of a PEDOT:PSS coated indium tin oxide (ITO) glass substrate. Aluminum (Al) electrodes were evaporated on the top, followed by annealing at 150 °C for 1 h. Device PCEs under simulated AM1.5 irradiation were $\sim 3\%$. Experimental measurements were performed at room temperature under nitrogen. Reflection-mode TAS data were collected either by using the Al electrode to reflect the probe beam (“device data”) or by directing the probe beam between the Al electrodes, and using a mirror placed directly behind the sample to reflect the beam back (“film data”).

Figure 1 shows a comparison of film and device TAS data

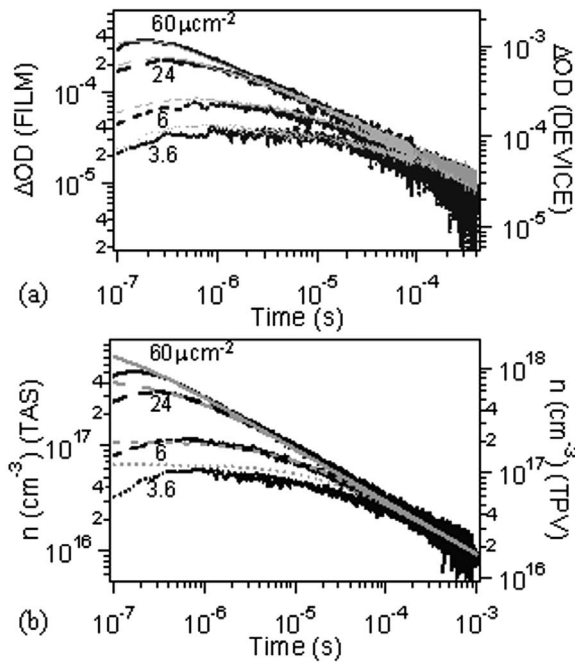


FIG. 1. (a) Comparison of reflection-mode TAS film (left—black) and device data (right—gray dashes) using a 520 nm pump and 980 nm probe. In both cases, a power-law decay $\Delta OD \propto t^{-\alpha}$ with $\alpha \sim 0.47$ is found at high pump intensities/long timescales. (b) Reflection-mode TAS device $n(t)$ data (left—black) compared to the simulated TAS data derived from TPV data (right—gray dashes).

collected as a function of excitation density under open-circuit conditions. The film data, and its dependence upon excitation density, are qualitatively similar to those we have reported previously for PPV/PCBM blend films, exhibiting a power law decay $\Delta OD \propto t^{-\alpha}$ with $\alpha \sim 0.47$. We have shown that this power-law behavior can be successfully simulated by a bimolecular recombination model incorporating an exponential tail of polaron trap states.^{11,12} We have shown that the exponent in such power-law decays for P3HT:PCBM films is dependent upon the P3HT regioregularity and film processing conditions, ranging between 0.3 and 0.7, attributed to variations in trap density.^{2,16} From Fig. 1(a), it is apparent that the thin film and device data show almost identical TAS decay dynamics (note there is a difference in signal amplitude attributed to optical interference effects influencing the device data). It can be concluded that the presence of the device Al electrode has no influence upon the polaron decay dynamics, and therefore that the device data are also consistent with this bimolecular recombination model. In general, the presence of the device electrodes is expected to generate electric fields between the device electrodes which might be expected to result in n and p both being position (x) dependent, thereby directly influencing the bimolecular recombination process given in Eq. (1). However, as the observed recombination dynamics appear to be independent of the presence of device electrodes, we conclude that any such spatial dependencies can be neglected for the decay dynamics addressed herein.

In addition to their potential influence of bimolecular re-

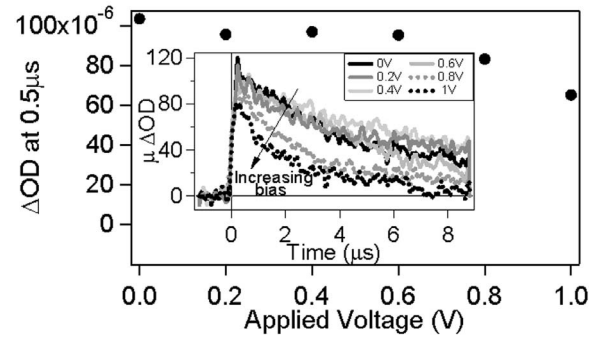


FIG. 2. Reflection-mode TAS data for a P3HT:PCBM device under different applied electrical bias. Over the voltage range 0–0.6 V (~ 1 sun V_{oc}), there is no significant variation in initial ($\sim 0.5 \mu s$) signal amplitude, indicating that geminate recombination losses do not strongly increase.

combination processes, device electric fields have been suggested to have a strong influence on geminate recombination losses.⁸ Such geminate recombination processes occur primarily on submicrosecond timescales,¹⁶ and would therefore, in the experiments reported herein, result in a loss of initial signal amplitude. In order to investigate this possibility further, the initial ($\sim 0.5 \mu s$) TAS amplitude was monitored in devices as a function of applied electrical bias. Low density excitation conditions were employed to ensure avoiding any possible effects of saturation or space charge screening. Typical data are shown in Fig. 2. It is apparent that in the range 0–0.6 V (~ 1 sun V_{oc}) there is no notable change in the initial signal amplitude. It can be concluded that over this voltage range geminate losses do not significantly change, and so the loss in photocurrent at an open circuit cannot be explained by this process. It should be noted that this observation does not imply that geminate recombination dynamics are in themselves negligible, but only that, for the P3HT:PCBM devices studied herein, any such losses are independent of device macroscopic electric field.¹⁶ At higher applied biases (above flat-band), we do observe a loss of initial signal amplitude; however, this is coupled with accelerated (μs) decay dynamics, and can most probably be attributed not to enhanced geminate recombination but rather either to rapid charge extraction by the device electrodes or accelerated bimolecular recombination.

The $\Delta OD(t)$ data shown herein can be converted directly into charge carrier dynamics $n(t)$ by using the Beer-Lambert law and employing a suitable value for the molar extinction coefficient (ϵ_M) for photogenerated polarons. For this purpose, the effective ϵ_M under the measurement conditions employed was determined to be $4 \pm 1 \times 10^4 \text{ M}^{-1}\text{cm}^{-1}$ by comparison of the initial ΔOD amplitude with an integrated short-circuit photocurrent transient for a device under the same low excitation density conditions.¹⁷ The resultant polaron density transients are plotted in Fig. 1(b). It is apparent that the densities monitored are in the range 10^{16} – 10^{18} cm^{-3} ,¹⁸ spanning the steady-state charge density reported for P3HT:PCBM devices at 1 sun V_{oc} (10^{17} cm^{-3}).¹⁴

We have recently presented an alternative small perturbation optoelectronic measurement of charge carrier dynamics in P3HT:PCBM solar cells, based upon transient photovolt-

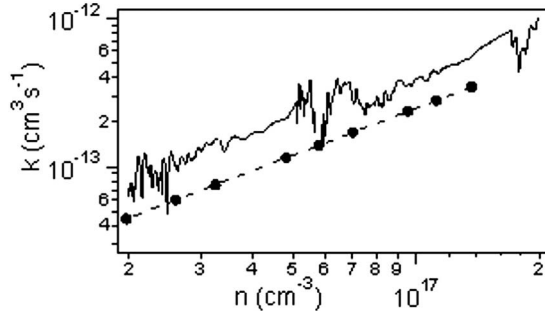


FIG. 3. Plots of bimolecular recombination coefficient, k , as a function of carrier concentration, n , calculated from measurements of TAS (bold) and TPV (dashed).

age (TPV) data obtained from devices held at an open circuit under continuous white light bias.¹⁴ Employing this methodology, we determined an empirical rate law for charge carrier decay dynamics in a P3HT:PCBM device at V_{oc} given by

$$\frac{dn}{dt} \approx - \frac{n^{1+\lambda}}{(1+\lambda)\tau_{\Delta n_0} n_0^\lambda}, \quad (2)$$

where λ , n_0 , and $\tau_{\Delta n_0}$ are experimentally determined constants and $(1+\lambda)$ corresponds to the empirical reaction order with respect to n . By integrating this rate law, we obtain an expression for the total carrier population dynamics $n(t)$, which can be used to simulate the $n(t)$ transients determined from the large perturbation ΔOD transients, assuming that both techniques are valid measurements of the underlying dynamics,

$$n(t) \approx n_{t=0} \left[1 + \frac{\lambda n_{t=0}^\lambda t}{(1+\lambda)\tau_{\Delta n_0} n_0^\lambda} \right]^{-1/\lambda}, \quad (3)$$

where $n_{t=0}$ corresponds to the initial charge density. This comparison is shown in Fig. 1(b), employing TPV data collected for the same device employed in the TAS studies ($\lambda \sim 2$, $n_0 = 1.1 \times 10^{15} \text{ cm}^{-3}$, $\tau_{\Delta n_0} = 0.17 \text{ s}$ and using $n_{t=0} (60 \mu\text{Jcm}^{-2}) = 2 \times 10^{18} \text{ cm}^{-3}$, which is scaled with excitation energy). It is striking that the charge carrier decay dynamics obtained from the large perturbation all optical TAS studies are in excellent agreement with the small perturbation optoelectronic TPV data. Given this agreement and the agreement between our film TAS decays, which we have previously assigned to bimolecular recombination, we conclude that the charge carrier dynamics observed by the TPV technique in devices under continuous bias irradiation at V_{oc} are also dominated by bimolecular recombination.

We now turn to calculation of the bimolecular rate constant for the decay dynamics shown in Fig. 1. Rearrangement of Eq. (1), employing the Beer-Lambert law to relate the observed optical density change ΔOD to charge density n and assuming charge neutrality ($n=p$), allows this coefficient to be determined directly from the TAS data (Fig. 3):

$$k = - \frac{d\Delta OD}{dt} \frac{2d\epsilon_M}{\Delta OD^2} \frac{1000}{N_A}, \quad (4)$$

where d is the device thickness and N_A is Avogadro's constant. Alternatively this rate constant can be calculated from consideration of the empirical rate law obtained from TPV transients given in Eq. (2):

$$k = \frac{n^{\lambda-1}}{(1+\lambda)\tau_{\Delta n_0} n_0^\lambda}. \quad (5)$$

Figure 3 shows the results of the calculations of the bimolecular rate constant k both from the large perturbation TAS data and from the TPV data reported in Ref. 14 plotted as a function of film charge density n . It is apparent that the two methodologies are in excellent agreement, both indicating that k is strongly carrier dependent, increasing almost linearly with increasing n ($k \propto n$), thereby resulting, for the typical device studied herein, in an overall third-order reaction rate law.

Our observation that the bimolecular rate constant is charge density dependent is in agreement with our previously reported microscopic model for this process incorporating an exponential tail of trapped hole states in the conjugated polymer, with thermally activated detrapping resulting in carrier concentration dependent recombination kinetics.¹² This model corresponds to a diffusional description of bimolecular recombination, where the rate constant is proportional to the effective polaron diffusion constant (or, by Einstein's relationship, the mobility), and this effective diffusion constant is charge density dependent. Carrier concentration dependent mobilities have also been reported from field-effect transistor (FET) mobility data for P3HT thin films.¹⁹ Our observation that k increases with n is important for device function, as it results in a strongly nonlinear increase in bimolecular recombination losses with increasing charge density.

The bimolecular rate constant k determined herein is significantly smaller (even for the highest charge densities studied) than that calculated for the Langevin recombination coefficient [$k_L = e(\mu_n + \mu_p)/\epsilon\epsilon_0$], where e is the electronic charge, ϵ (ϵ_0) is the relative (absolute) dielectric permittivity, and μ_n (μ_p) is the electron (hole) mobility.⁵ Time-of-flight (TOF) studies of similar blend films indicate polaron mobilities on the order of $\sim 10^{-4} \text{ cm}^2 \text{ s}^{-1} \text{ V}^{-1}$ (Ref. 2), which predict $k_L = 10^{-10} \text{ cm}^3 \text{ s}^{-1}$, 2–3 orders of magnitude higher than the values of k determined herein (see Fig. 3). This conclusion is consistent with previous double injection and integral mode TOF studies.^{4,5} The relatively low value for the observed bimolecular rate constant has been suggested to result from phase separation of the polymer and PCBM components of the film. Whatever its origin, the observation that $k \ll k_L$ is critical to reducing bimolecular losses and enabling efficient device performance.

We have shown above that the charge carrier decay dynamics in the P3HT:PCBM studied herein under open-circuit conditions are dominated by bimolecular recombination. We note that the observed strong carrier dependence of these bimolecular losses is consistent with such bimolecular recombination losses being relatively unimportant at a short

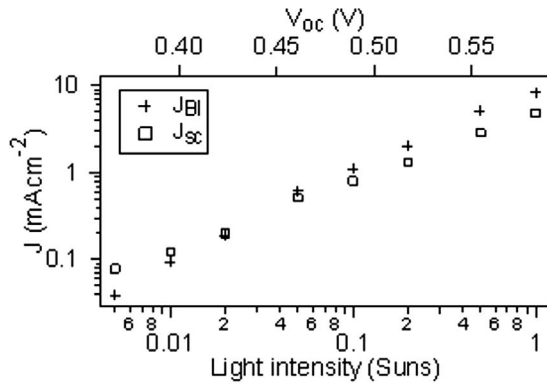


FIG. 4. Comparison of the calculated bimolecular recombination flux at open-circuit J_{BI} (crosses) with the corresponding short-circuit photocurrent J_{sc} (open squares).

circuit, where charge extraction by the electrodes results in significantly lower charge carrier densities. We turn now to quantification of J_{BI} , the bimolecular recombination flux at V_{oc} :

$$J_{\text{BI}} = -knpde. \quad (6)$$

J_{BI} acts in the opposite sense to the photocurrent, hence reducing the net current density extracted under operating conditions. For determination of J_{BI} , we use values for n , p determined from differential charging¹⁴ and charge extraction techniques, TPV data for k , assuming $n=p$ and neglecting (see above) any spatial dependence of n or p . This recombination flux is compared in Fig. 4 against the short-circuit photocurrent J_{sc} measured under the same light condi-

tions. We find that over the whole range of light intensities studied, J_{BI} at V_{oc} is approximately equal to J_{sc} , further supporting our conclusion that the primary factor resulting in loss of photocurrent output at an open circuit is bimolecular recombination.

Previous studies of the factors limiting the open-circuit voltage of bulk heterojunction solar cells have shown a correlation between V_{oc} and the separation of the donor highest occupied molecular orbital (HOMO) and acceptor lowest unoccupied molecular orbital (LUMO) levels.⁹ The results we report herein suggest this dependence may originate, at least in part, from bimolecular recombination losses, with shifts in HOMO/LUMO levels modulating charge carrier densities and thereby the bimolecular recombination flux J_{BI} . We note this correlation has previously been related to dark current diode losses limiting V_{oc} , suggesting that the dark current may (over the conditions studied herein) originate from a bimolecular recombination process. In any case, given the relatively modest voltage output of P3HT:PCBM solar cells (0.6 V compared to the blend electronic band gap of 1.1 eV), we conclude that minimization of such bimolecular losses is likely to be essential to improve the voltage output, and therefore power conversion efficiency, of P3HT:PCBM solar cells. For example, the data we present herein indicating that a reduction of the bimolecular rate constant by 10 will result in a ten-fold reduction in J_{BI} and thus, from Fig. 4, for a constant light intensity, approximately a 0.1 V increase in device open-circuit voltage.

Financial support from EPSRC-GB, DTI and BP Solar, and P3HT synthesis and financial support from Merck Chemicals are gratefully acknowledged.

*j.durrant@imperial.ac.uk

¹J. Peet, J. Y. Kim, N. E. Coates, W. L. Ma, D. Moses, A. J. Heeger, and G. C. Bazan, *Nat. Mater.* **6**, 497 (2007).

²Y. Kim, S. Cook, S. M. Tuladhar, S. A. Choulis, J. Nelson, J. R. Durrant, D. D. C. Bradley, M. Giles, I. McCulloch, C. Ha, and M. Ree, *Nat. Mater.* **5**, 197 (2006).

³A. J. Mozer, G. Dennler, N. S. Sariciftci, M. Westerling, A. Pivrikas, R. Osterbacka, and G. Juska, *Phys. Rev. B* **72**, 035217 (2005).

⁴G. Juska, G. Sliuzys, K. Genevicius, K. Arlauskas, A. Pivrikas, M. Scharber, G. Dennler, N. S. Sariciftci, and R. Osterbacka, *Phys. Rev. B* **74**, 115314 (2006).

⁵A. Pivrikas, G. Juska, A. J. Mozer, M. Scharber, K. Arlauskas, N. S. Sariciftci, H. Stubb, and R. Osterbacka, *Phys. Rev. Lett.* **94**, 176806 (2005).

⁶L. J. A. Koster, V. D. Mihailetchi, and P. W. M. Blom, *Appl. Phys. Lett.* **88**, 093511 (2006).

⁷L. J. A. Koster, V. D. Mihailetchi, R. Ramaker, and P. W. M. Blom, *Appl. Phys. Lett.* **86**, 123509 (2005).

⁸R. A. Marsh, C. Groves, and N. C. Greenham, *J. Appl. Phys.* **101**, 083509 (2007).

⁹M. C. Scharber, D. Wuhlbacher, M. Koppe, P. Denk, C. Waldauf, A. J. Heeger, and C. L. Brabec, *Adv. Mater. (Weinheim, Ger.)* **18**, 789 (2006).

¹⁰L. J. A. Koster, E. C. P. Smits, V. D. Mihailetchi, and P. W. M.

Blom, *Phys. Rev. B* **72**, 085205 (2005).

¹¹I. Montanari, A. F. Nogueira, J. Nelson, J. R. Durrant, C. Winder, M. A. Loi, N. S. Sariciftci, and C. Brabec, *Appl. Phys. Lett.* **81**, 3001 (2002).

¹²J. Nelson, *Phys. Rev. B* **67**, 155209 (2003).

¹³B. C. O'Regan and J. R. Durrant, *J. Phys. Chem. B* **110**, 8544 (2006).

¹⁴C. G. Shuttle, B. O'Regan, A. M. Ballantyne, J. Nelson, D. D. C. Bradley, J. de Mello, and J. R. Durrant, *Appl. Phys. Lett.* **92**, 093311 (2008).

¹⁵R. Osterbacka, C. P. An, X. M. Jiang, and Z. V. Vardeny, *Science* **287**, 839 (2000).

¹⁶H. Ohkita, S. Cook, Y. Astuti, W. Duffy, S. Tierney, W. Zhang, M. Heeney, I. McCulloch, J. Nelson, D. D. C. Bradley, and J. R. Durrant, *J. Am. Chem. Soc.* **130**, 3030 (2008).

¹⁷See EPAPS Document No. E-PRBMDO-78-097831 for details on determination of the effective P3HT⁺ polaron molar extinction coefficient. For more information on EPAPS, see <http://www.aip.org/pubservs/epaps.html>.

¹⁸We note that due to the high laser intensities employed the values of n observed on the μs -ms scale will include the effects of the fast trap-free bimolecular decay kinetics observed on earlier timescales (Ref. 11).

¹⁹C. Tanase, E. J. Meijer, P. W. M. Blom, and D. M. de Leeuw, *Phys. Rev. Lett.* **91**, 216601 (2003).